Optimizing Parapets for Rooftop Wind Safety Using CFD Simulations and Sensitivity Analysis

Chao Lin[1*], *Hideki* Kikumoto[1], *Yasutomo* Takakuwa[1], and *Ryozo* Ooka[1]

[1] Institute of Industrial Science, The University of Tokyo, 4-6-1 Komaba, Meguro-ku, Tokyo, 153-8505, Japan

Abstract. The complex rooftop wind environment, dominated by flow separation at building edges, presents safety challenges for rooftop activities such as roof gardens and urban air mobility (UAM) operations. This study investigates the wind sheltering performance of rooftop parapets on a 40 m-high isolated building using computational fluid dynamics (CFD) simulations, with the wind direction perpendicular to the windward building face. A total of 729 simulations are conducted, systematically varying the parapet height (0–4 m in 1 m intervals) and porosity (solid or 40%) across the upwind, two sides, and downwind edges. Configurations of the two side parapets are kept identical across all cases. CFD results for solid parapets are validated against wind tunnel measurements at a 1:200 scale, showing good agreement. Wind conditions are evaluated using volume-averaged statistics within the 0–2 m height range above the rooftop surface, corresponding to the typical occupied zone during rooftop use. Results reveal that different parapet configurations can cause rooftop wind speed (WS) to vary between a 50% reduction and a 12% increase, turbulent kinetic energy (TKE) between a 72% reduction and a 2% increase, and total kinetic energy (total KE) between a 65% reduction and a 6% increase. Global sensitivity analysis using the Sobol method identifies the upwind and downwind parapet heights as the dominant parameters affecting WS, while the height and porosity of the upwind parapet primarily influence TKE and total KE. Specifically, a porous upwind parapet with height ≤ 2 m combined with solid side parapets proves most effective to reduce WS. A tall solid upwind parapet (≥ 3 m) paired with solid side parapets is recommended to minimize TKE and total KE. These findings offer guidance for optimizing rooftop parapet design to enhance wind safety in rooftop usage scenarios.

Keywords. Rooftop, Wind speed, Parapet, CFD, Optimization

1 Introduction

Urban rooftop environments have become increasingly critical for the deployment of Urban Air Mobility (UAM) operations [1]. As rooftops are expected to serve as takeoff and landing sites, ensuring safe wind conditions is essential for reliable UAM services. However, rooftop airflow is highly sensitive to building geometry, particularly the presence of parapets. While previous studies have shown that parapets significantly alter flow separation, recirculation zones, and turbulence generation [2, 3], yet the combined effects of parapet height and porosity on rooftop wind environments remain insufficiently understood. Moreover, the interactions among multiple parapet parameters create a complex design space that has not been comprehensively quantified. To address these gaps, this study systematically investigates the rooftop wind environment under a large number (>700) of parapet configurations using computational fluid dynamics (CFD) simulations. The spatial distributions of time-averaged flow fields and turbulent kinetic energy are discussed for the representative parapet configurations. In addition, a global sensitive analysis is conducted to identify the most influential parapet parameters affecting the flow field. Finally, the common characteristics of parapet configurations that lead to optimal (low-speed) and adverse (high-speed) wind environments are identified.

2 Simulation settings

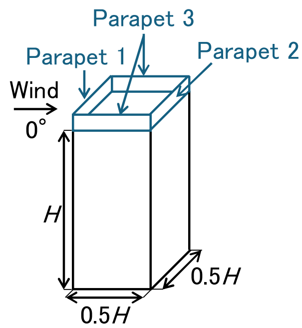

Fig. 1. Schematic of building and parapet model.

* Corresponding author: c-lin415@iis.u-tokyo.ac.jp

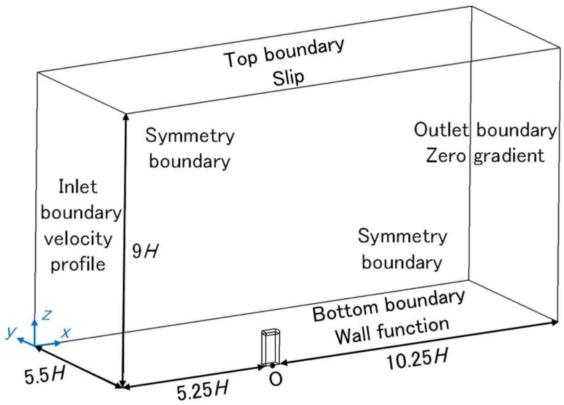

Fig. 2. Simulation domain.

Figure 1 shows the 1:1:2 building model with the building height of H = 40 m. Parapets were installed along all roof edges. Parapets 1, 2 and 3 denote upwind, downwind and side parapets, respectively. Their heights and porosities are denoted as h1, h2, h3 and p1, p2, p3. The parapet height was varied from 0 to 4 m at increments of 1 m, and the parapet porosity was set to either solid or 40%. A total of 729 combinations of parapet height and porosity were examined in this study.

Figure 2 shows the simulation domain and boundary conditions. The domain comprised 16*H*, 5.5*H*, and 9*H* in the streamwise (*x*), spanwise (*y*), and vertical (*z*) directions, respectively. Owing to the theoretical symmetry of the time-averaged flow field in the *y* direction, only half of the domain was simulated.

Figure 3 shows inflow conditions. The solid line indicates a power-law fit with an exponent of 0.22. The wind velocity at 20 m was set as 10 m/s, representing a strong-wind condition that may pose hazards to UAM operation. Flow fields were computed using OpenFOAM v2012, solving the transport equations of the steady-state RANS model with the realizable k–ε turbulence closure.

The parapets were modeled as having zero thickness. The aerodynamic effects of porous parapets were represented using a one-dimensional simplification of the porous-media model, called the 'porous jump' model. The pressure-loss coefficient of the porous parapet was taken as 11.7, following the measurements reported by Tominaga and Shirzadi (2022) [4].

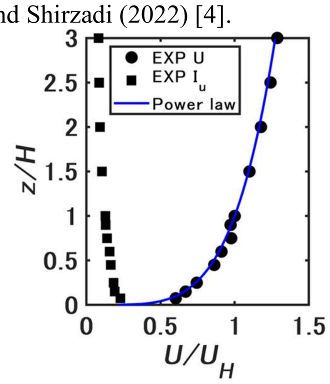

Fig. 3. Inflow wind velocity and turbulence intensity.

3 Results and discussion

3.1 Validation

The prediction accuracy of the CFD simulations was validated against wind tunnel measurements [2]. In the experimental, a small recirculation zone was observed in the no-parapet case (Figures 4(a)), whereas the presence of parapets significantly enlarged the recirculation region (Figures 4(c)). The CFD results exhibited generally good agreement with the experimental data. Specifically, although the CFD simulations slightly underestimated the size of the recirculation zone in the no-parapet case (Figures 4(b)), they accurately reproduced both the recirculation extent and the vortex center locations for the parapet configurations (Figures 4(d)). Overall, the predictive performance of the CFD model is considered satisfactory for the objectives of this study.

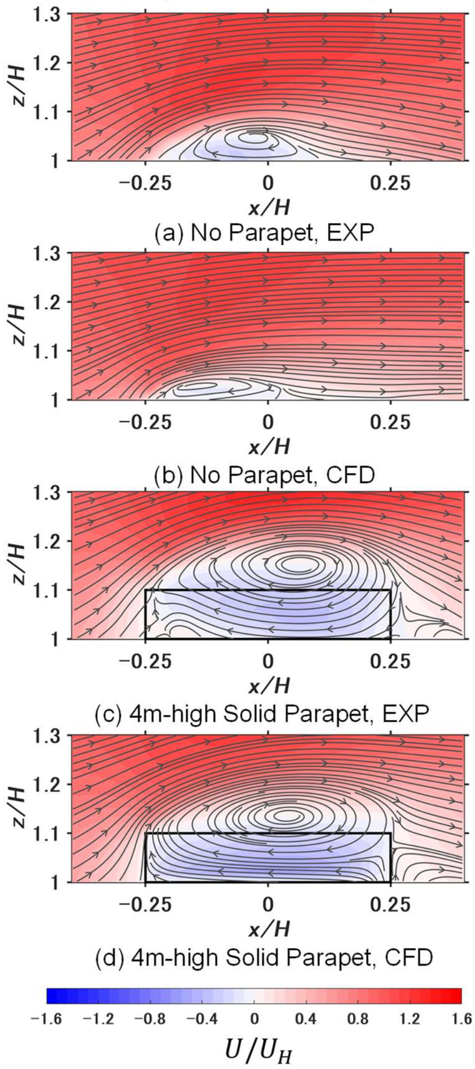

Fig. 4. Distributions of time-averaged *x*-direction wind velocity *U* in the vertical plane *y*/*H* = 0 based on wind tunnel experiment and CFD simulations.

3.2 Flow fields

The rooftop time-averaged wind speed (WS), turbulent kinetic energy (TKE) and total kinetic energy (total KE, $E = 0.5\ WS^2 + k$) under various parapet configurations are analyzed. The target region for evaluating the parapet effect was defined as the volume within 0–2 m above the rooftop surface, corresponding to the typical occupied zone.

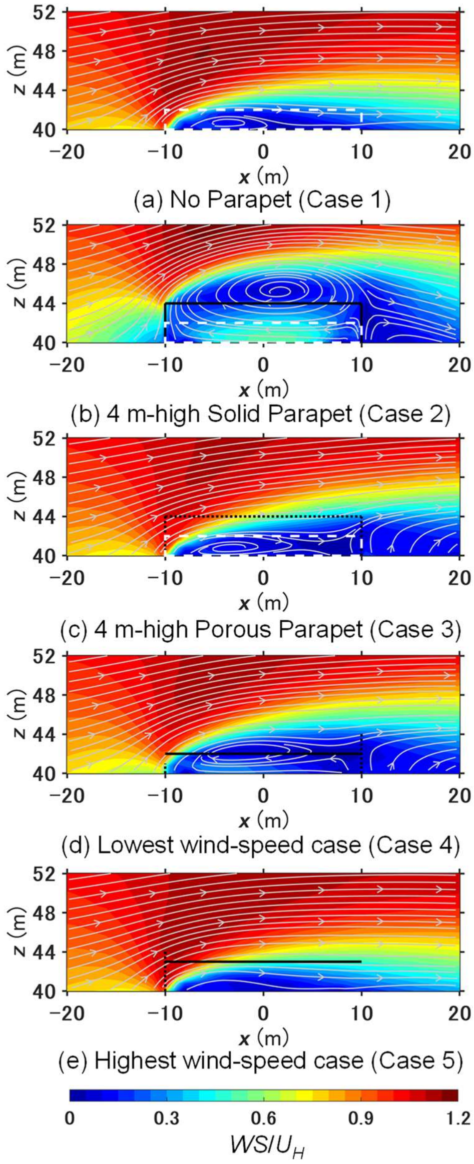

Fig. 5. Distributions of time-averaged wind speed in the vertical plane *y*/*H* = 0. Solid and dot lines refer to solid and porous parapets. The location of lines refers to parapet height. Dash lines refer to the evaluation area.

Seven representative cases are discussed in this section. Among them, three simple configurations serve as baseline cases: Case 1 (no-parapet), Case 2 (tallest solid parapet), and Case 3 (tallest porous parapet). Cases 4 and 5 represent the configurations with the lowest and highest WS within the target region, respectively. Similarly, Cases 6 and 7 identify the configurations with the lowest and highest TKE.

Figure 5 shows the WS distributions in the vertical plane *y*/*H* = 0 for different parapet configurations. Table 1 summarizes the volume-averaged statistics for the targe region. For basic cases, Case 1 shows a low-WS zone near the roof surface because of the separation flow (Figure 5(a)). Although Case 2 (Figure 5(b)) shows a larger size of low WS zone than Case 3 (Figure 5(c)), the WS reduction rate (-15%) is smaller than Case 3 (-32%). This is because the solid parapet induces a strong recirculation flow near the roof surface. Compared to Case 1, the lowest WS case (Case 4) and the highest WS case (Case 5) decreased 50% and increased 12% of volume-averaged WS, respectively. Case 4 is characterized as a low porous upwind-parapet, a high porous downwind-parapet and a solid side parapet. Case 5 is characterized as a high porous upwind-parapet, no downwind parapet and a solid side parapet.

Table 1. Volume-averaged statistics within the 0–2 m height range above the rooftop surface with different parapet parameters. Numbers indicate change rate from Case 1. For *p1*, *p2* and *p3*, S means solid parapet, P means porous parapet and N means no parapet. The WS/U_H, k/U_H^2 and E/U_H^2 for Case 1 are 0.35, 0.08 and 0.17, respectively.

Case	1	2	3	4	5	6	7
h1 (m)	0	4	4	1	4	4	4
h2 (m)	0	4	4	4	0	0	0
h3 (m)	0	4	4	2	3	4	1
p1	N	S	P	P	P	S	P
p2	N	S	P	P	N	N	N
p3	N	S	P	S	S	S	P
WS/U_H change (%)	-	-15	-32	-50	12	-25	5
k/U_H^2 change (%)	-	-70	-2	-18	-2	-72	2
E/U_H^2 change (%)	-	-56	-19	-46	12	-65	6

Figure 6 shows the TKE distributions in the same vertical plane. For the baseline cases, Case 1 produces a high-TKE region near the upwind roof edge due to flow separation (Figure 6(a)). Case 2 demonstrates that a solid parapet shifts and expands the high-TKE region toward the parapet's top edge (Figure 6(b)). In contrast, Case 3 increases TKE near the downwind parapet compared to Case 1 (Figure 6(c)). Case 6 (the lowest-TKE case) achieves a 72% reduction in volume-averaged TKE relative to Case 1. This is accomplished by utilizing tall solid parapets along the upwind and side edges, which effectively lift the shear layer and high-TKE region upward, away from the rooftop surface. Conversely, Case 7 (the highest-TKE case) slightly increases the volume-averaged TKE by incorporating a tall porous upwind parapet.

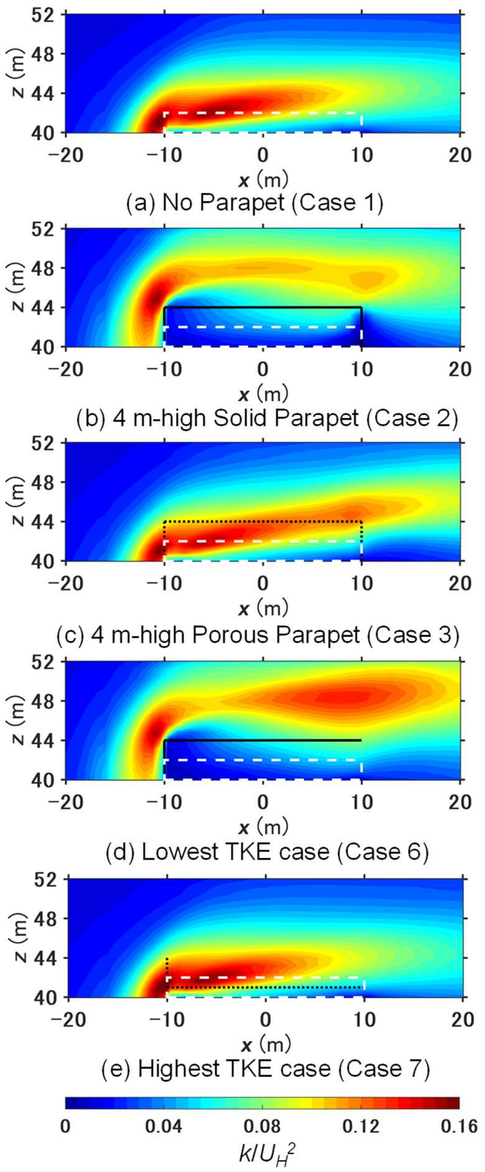

Fig. 6. Distributions of turbulent kinetic energy in the vertical plane $y/H = 0$. Line meanings refer to Figure. 5.

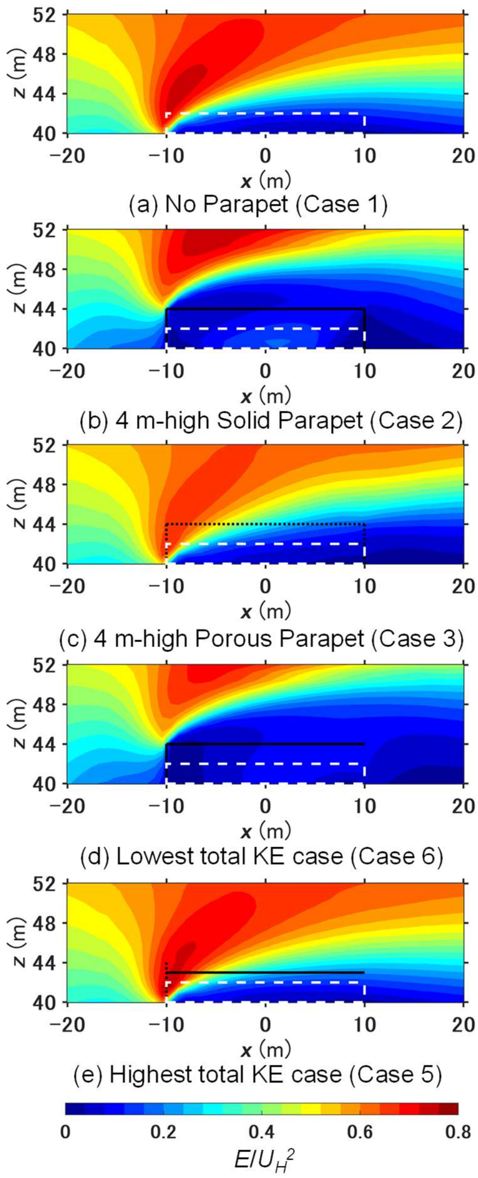

Fig. 7. Distributions of total kinetic energy in the vertical plane $y/H = 0$. Line meanings refer to Figure. 5.

Figure 7 shows the total KE distributions in the same vertical plane. The distribution in Case 1 is similar to its WS profile (Figure 5(a)), characterized by high total KE near the upwind building corner. Case 2 significantly decreases total KE below the parapet height, resulting in a 56% reduction within the target zone. However, Case 3 only reduced 19% of total KE, indicating that the porous parapet is not effective in reducing TKE as shown in Figure 6(c). Notably, Case 6, previously identified as the lowest-TKE case, also yields the minimum total KE (a 65% reduction), highlighting the critical role of upwind solid parapets. On the other hand, Case 5, the highest WS case, is also the highest total KE case (a 12% increase). This suggests that upwind porous parapets alone cannot sufficiently mitigate total KE, requiring the addition of a downwind parapet for enhanced performance.

3.3 Statistical analysis of parapet parameters

To provide the best practice for parapet design, it is important to identify the key parameters governing the rooftop wind environment. First, a global sensitivity analysis of parapet parameters was conducted using the first and total order of Sobol indices [5]. Results indicate that *h1*, *h2* and *p1* are the primary factors affecting WS (Figure 8 (a)). For TKE and total KE, *p1* and *h1* are identified as dominant factors. However, it should be noted that the rooftop wind environment cannot be optimized by adjusting these variables in isolation. Consequently, the prevailing morphological features of the configurations yielding the most and least favorable wind conditions among the 729 cases were analyzed.

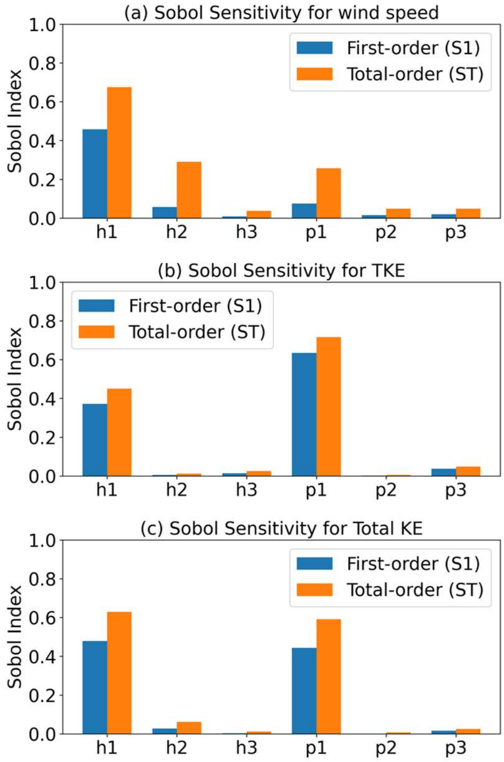

Fig. 8. Sobol indices for volume-averaged (a) time-averaged wind speed, (b) turbulent kinetic energy and (c) total kinetic energy.

Figure 9 shows the parapet parameter distributions for (a) the 20 cases with lowest WS and (b) the 20 cases with highest WS. The low-WS configurations consistently feature a porous upwind parapet (height ≤ 2 m) coupled with solid side parapets. In contrast, high-WS cases are characterized by the absence of an upwind parapet or the use of a tall porous one, typically compounded by the lack of a downwind parapet.

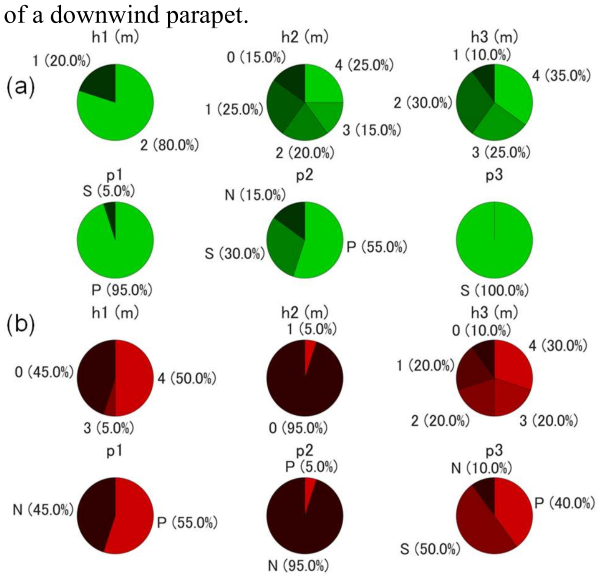

Fig. 9. Parapet parameter distributions for (a) the 20 lowest WS cases and (b) the 20 highest WS cases.

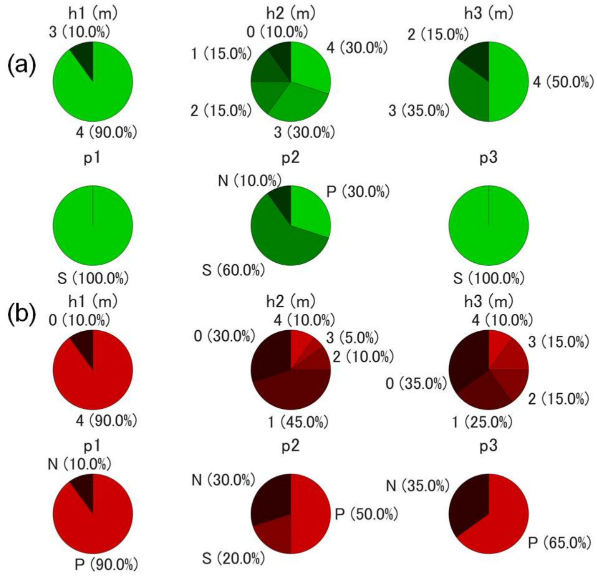

Fig. 10. Parapet parameter distributions for (a) the 20 lowest TKE cases and (b) the 20 highest TKE cases.

Figure 10 shows the parameter distributions for (a) the 20 lowest-TKE cases and (b) the 20 highest-TKE cases. The low-TKE group exhibits a common pattern: a solid upwind parapet exceeding 3 m in height combined with solid side parapets. In contrast, high-TKE environments are generally associated with configurations featuring tall porous upwind parapets, particularly when side parapets are either porous or entirely absent.

Figure 11 shows the distributions for (a) the 20 lowest and (b) the 20 highest total KE cases. Configurations with minimal total KE generally incorporate both high solid upwind and side parapets. On the other hand, the highest total KE cases mirror the trends observed for high-WS conditions (Figure 8(b)), defined by the omission of upwind parapets or the presence of tall porous ones,

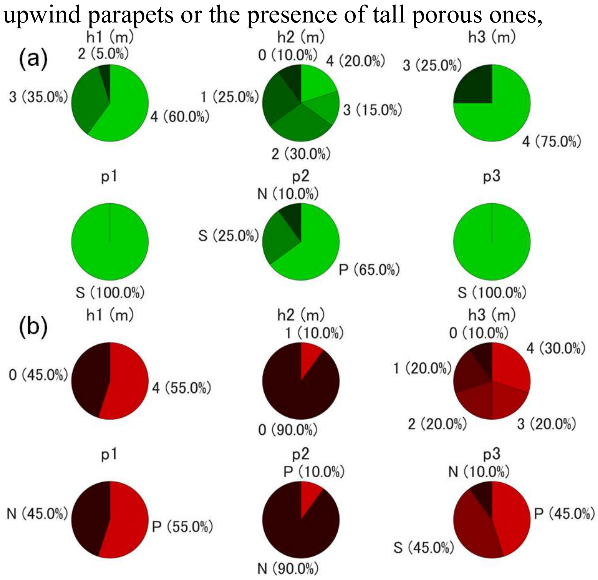

Fig. 11. Parapet parameter distributions for (a) the 20 lowest total KE cases and (b) the 20 highest total KE cases.

alongside the absence of downwind protection.

4 Conclusions

This study systematically investigated the influence of parapet height and porosity on rooftop wind environments using a dataset of 729 configurations evaluated via CFD simulations and global sensitivity analysis. The key findings are summarized as follows:

(1) The results demonstrate that parapets can substantially modify both wind speed and turbulence intensity above rooftop surfaces. Solid parapets tend to enhance recirculation and reduce wind speed near the surface, whereas porous parapets more effectively moderate separation but may increase turbulence in localized regions.

(2) Global sensitivity analysis reveals that upwind parapet height (*h1*), side parapet height (*h2*), and upwind porosity (*p1*) are the primary drivers governing rooftop wind speed (WS). While *h1* and *p1* are especially important to turbulent kinetic energy (TKE) and total kinetic energy (total KE). These results indicate that the rooftop environment is a product of complex parameter interactions that necessitate a holistic design approach.

(3) For minimizing WS, a porous upwind parapet with height ≤ 2 m combined with solid side parapets proves most effective. To minimize TKE and total KE, a tall solid upwind parapet (≥ 3 m) paired with solid side parapets is recommended, as this configuration effectively lifts the shear layer away from the UAM operational zone.

(4) High-WS results are mainly observed when the upwind parapet is absent or replaced by a tall porous parapet, particularly in the absence of a downwind parapet. High-TKE results are primarily linked to configurations with tall porous upwind parapets, especially when the side parapets are porous or entirely omitted. The cases with the highest total KE exhibit patterns similar to those of the high-WS cases, characterized by the absence of an upwind parapet or the use of a tall porous one, together with insufficient downwind shielding.

These findings provide quantitative design guidelines for optimizing rooftop vertiports, ensuring safer and more reliable Urban Air Mobility (UAM) operations through strategic parapet configuration. However, it should be recognized that the conclusions may vary based on the evaluation area due to significant spatial variations in wind distribution. As a future prospect, we aim to employ high-resolution Large Eddy Simulation to better resolve the multi-scale turbulence associated with UAM. A primary objective will be the assessment of safety-critical indicators, including instantaneous wind velocity fluctuations and gust occurrences, which are vital for ensuring the structural and operational integrity of UAM systems.

Acknowledgements
This work was supported by the Japan Society for the Promotion of Science (JSPS) KAKENHI Grant Number 24K17398 and the Kajima Foundation's General Research Grants.

Reference

1. H. Jia, C. Lin, M. Iwabuchi, H. Kikumoto, Ten questions concerning urban wind environments for the safe utilization of urban air mobility. Build Environ **290**, 114136 (2026).
https://doi.org/10.1016/j.buildenv.2025.114136
2. C. Lin, R. Ooka, Y. Takakuwa, H. Kikumoto, Wind tunnel study of Parapet effects on rooftop wind environment with implications for safe urban-air-mobility operations. Build Environ **284**, 113509 (2025).
https://doi.org/10.1016/j.buildenv.2025.113509
3. C. Lin, R. Ooka, Y. Takakuwa, H. Kikumoto, Rooftop wind environment with parapets under upwind building sheltering: A wind tunnel study with implications for urban-air-mobility safety. Build Environ **287**, 113854 (2026).
https://doi.org/10.1016/j.buildenv.2025.113854
4. Y. Tominaga, M. Shirzadi,. RANS CFD modeling of the flow around a thin windbreak fence with various porosities: Validation using wind tunnel measurements. J. Wind Eng. Ind. Aerodyn. **230**, 105176 (2022).
https://doi.org/10.1016/J.JWEIA.2022.105176
5. A. Saltelli, P. Annoni, I. Azzini, F. Campolongo, M. Ratto, S. Tarantola, 2010. Variance based sensitivity analysis of model output. Design and estimator for the total sensitivity index. Comput Phys Commun **181**, 259–270 (2010).
https://doi.org/10.1016/J.CPC.2009.09.018